Article

Research on the Optimization of the Operating Parameters of Methane Carbon Dioxide Reforming Using the Response Surface Methodology

Xing Huang [1], Zhengguo Lv [1], Xin Yao [1,*], Yang Liu [2,*], Yuhe Wang [1] and Sijia Zhu [1]

[1] College of Metallurgy and Energy, North China University of Science and Technology, Tangshan 063210, China; minthx@163.com (X.H.); lv2021_hblg@163.com (Z.L.); 15175568273@163.com (Y.W.); 17730506490@163.com (S.Z.)
[2] Health Center, North China University of Science and Technology, Tangshan 063210, China
* Correspondence: yaoxin_0129@163.com (X.Y.); liuyangineur@outlook.com (Y.L.)

Abstract: In order to reduce the production cost of the methane carbon dioxide reforming reaction, and improve its actual production efficiency, in this paper, the optimal working parameters of the methane carbon dioxide reforming reaction are studied. The influence of different factors on methane conversion is studied via a single-factor numerical simulation analysis and the response surface methodology. Firstly, a numerical model of the methane carbon dioxide reforming reaction is established using Ansys Chemkin Pro software to analyze the influence of single factors (reactor temperature, reaction pressure, gas velocity) on methane conversion rate; secondly, the response surface model with the methane conversion rate as the response value is established using the BBD (Box–Behnken design) method; and finally, the order of influence of each variable on methane conversion and the optimal reaction conditions are determined using the response surface method. The factors are listed in order of their influence on methane conversion as follows: reactor temperature > pressure > speed. The results show that when the temperature is 1135.114 K, the pressure is 0.103 MPa and the speed is 10slpm, the methane conversion rate is 93.7018%. In this paper, a method is adopted in which chemical reaction process simulation and numerical results prediction are combined, significantly reducing the simulation time and improving the calculation efficiency and accuracy, thus being of considerable scientific significance and theoretical value.

Keywords: methane carbon dioxide reforming; chemkin simulation; response surface methodology; parameter optimization; BBD

1. Introduction

The continuous development of human society is inseparable from the assistance of industry, with the importance of the iron and steel metallurgy industry being self evident. However, with the vigorous development of the metallurgical industry, we will be presented with an increasing number of problems. The most obvious of these are related to the environment. The earth's natural environment is the basic resource for human development. Therefore, protecting the earth's environment is to protect the future of mankind. Therefore, we should actively participate in the resolution of environmental issues. At present, the work in the steel field has achieved its aims of increasing production capacity and improving efficiency, with coal having been used as the main energy source and reducing agent [1]. However, the contradiction between the reality of high emissions and high energy consumption and the green development of the environment has become increasingly prominent. From the perspective of energy efficiency, the technology for metallurgical processes is close to perfection, and is constantly approaching the limits of carbon reduction potential. Therefore, it is urgent to find low-carbon and green metallurgical methods [2].

The emergence of hydrogen metallurgy has provided hope for the possibility of realizing a low-carbon green transformation, upgrading the steel industry [3]. Some studies [4,5] have reported that the only means by which CO_2 emissions can be reduced in ironmaking is to increase the use of H_2. Conversely, H_2 reduces iron ore more efficiently than CO, because H_2 has smaller molecules, and is easily permeable to iron ore [6,7]. The rational use of H_2 in ironmaking processes could have a significant impact on reducing energy use and CO_2 emissions. The world's largest steel-producing nations incorporated this into their national development strategies at the beginning of the 21st century. Promoting the transformation from "carbon metallurgy" to "hydrogen metallurgy" is expected to further accelerate the green, low-carbon transformation, and help achieve the "win–win" situation of the development of hydrogen energy and the steel industry, and whether hydrogen metallurgy can play a key supporting role in achieving carbon neutrality in the steel industry depends to some extent on whether green hydrogen can be used to obtain a stable and economically viable supply. However, there are still many significant limitations, especially in the development of hydrogen production [8]. Almost all hydrogen is produced from fossil fuels, accounting for the consumption of 6% of global natural gas and 2% of global coal, and producing 830 million tons of CO_2 emissions [9]. Therefore, the production of green hydrogen through the use of renewable energy is the way of the future.

At the same time, with the development of society and the economy, while there is an increasing demand for energy, the main source of energy worldwide is still the burning of fossil fuels, resulting in increased emissions of the greenhouse gas carbon dioxide (CO_2), exacerbating global warming. In order to stop the effect of global warming effect [10], attention is being turned to limiting the emissions of two greenhouse gases, methane and carbon dioxide. Therefore, the emergence of reforming methane carbon dioxide into hydrogen has brought about a new dawn in achieving the green transformation of the iron and steel metallurgy industry and at the same time curbing global warming. Methane (CH_4) is the simplest hydrocarbon compound, and is widely used and abundant. CH_4 in nature is mostly found in natural gas, coal mines and biogas. However, CH_4 itself is chemically stable, and it is difficult to directly convert it into other hydrocarbon compounds. In contrast, indirect conversion to produce liquid hydrocarbons is more convenient [11]. At the same time, the stability of carbon dioxide itself makes it possible to use carbon dioxide gas as a reactant in large quantities [12–14]. As a result, attention is turning to limiting methane and carbon dioxide emissions, and there is a renewed wave of research on methane carbon dioxide reforming [15–22].

Methane carbon dioxide reforming has the following advantages: simple process flow and low equipment requirements; easy access to raw materials; and the whole production process is green and emission free [23]. The conversion rate of raw materials can reach close to 100%, and the ratio of hydrogen and carbon monoxide in the produced syngas is 1:1, and these can be used directly as raw materials in Fischer–Tropsch synthesis [24,25]. Combined with the current status of industrial development and global environmental trends, the green and easy availability of the raw materials required for methane carbon dioxide reforming could not only reduce the world's carbon emissions, but the syngas could be also directly used as the feed gases for producing substitutes for oil for use as fuel [22,26]. These advantages once again confirm the fact that methane carbon dioxide has great potential for development. Although methane dry reforming has obvious advantages over other methane indirect conversion methods, methane carbon dioxide reforming also has disadvantages, and its industrial maturity is still insufficient. The main disadvantage is that the higher bond energy of the carbon oxygen bond causes carbon dioxide to be very stable, so higher energy is required to drive the reaction, which determines that the reaction can only obtain higher hydrogen and carbon monoxide yields at higher reaction temperatures (usually > 750 °C) [19]. This also placed greater requirements on the catalyst added during the methane carbon dioxide reforming reaction.

The most commonly used catalysts in methane carbon dioxide reforming reactions are nickel-based catalysts. Although the use of precious metals as catalysts provides better

catalytic effect (reactant conversion rate, generated yield) and better catalytic performance (long life, high carbon deposition resistance), their higher price and recovery cost after the reaction condemn them to the fate of not being used in actual production in the real world. Therefore, researchers have focused their attention on non-noble metal catalysts. Nickel-based catalysts can be used, and are the most commonly used catalysts, which is inseparable from nickel's strong ability to break carbon hydrogen bonds [27]. However, nickel-based catalysts are easily inactivated by carbon deposition at high temperatures [28]. Therefore, improving the anti-carbon-deposition ability of nickel-based catalysts is the main research direction of catalysts for the methane carbon dioxide reforming reaction. SHAMSUDDIN et al. [29] and LIN et al. [30] found that changing the loading of the active components on the catalyst could improve the anti-carbon-deposition performance of the catalyst. SHAMSUDDIN et al. [29] prepared NiO/Talc catalysts with 5%, 10% and 15% loads, respectively. Among them, the 10% NiO/Talc catalyst not only ensured high dispersion, but also exhibited strong anti-carbon-deposition performance. JING et al. [31] and JEONG et al. [32] found that adding additives to the catalyst could also improve the anti-carbon-deposition performance of the catalyst. JING et al. [31] added MgO to the Ni/SiO_2 catalyst and found that the electron density in the catalyst increased, and the dissociation ability of carbon dioxide was enhanced, thereby improving the anti-carbon-deposition performance. JEONG et al. [32] added Mg to the Ni/HY catalyst and found that the dispersion of the active components was improved, alleviating the sintering and carbon deposition phenomena.

To date, although many scholars have conducted large and detailed studies on the methane carbon dioxide reforming reaction, these studies have mainly focused on controlling the different variables, and research on methane carbon dioxide reforming has largely been based on single-factor analysis [33–37]. However, in actual production activities, there are often a variety of factors that interact, playing their roles at the same time, rather than a simple single factor that affects the methane conversion rate of the methane carbon dioxide reforming reaction, and how to control production costs while improving methane conversion should be considered from a more macro perspective. Therefore, the Box–Behnken Design (BBD) model [38] was selected, implemented via the response surface methodology, to analyze the thermodynamic design of the methane carbon dioxide reforming reaction, and a response surface model was built according to each response value on the basis of multi-factor coupling analysis; finally, a calculation formula able to reflect the relationship between the influencing factors and the response value was fitted, in order to provide a theoretical basis for the optimization of the thermal parameters of methane carbon dioxide reforming. In this paper, a method is adopted in which chemical reaction process simulation and numerical result prediction are combined, resulting in a significantly reduced simulation time and improved calculation efficiency and accuracy, thus being of considerable scientific significance and theoretical value.

2. Modeling

In this paper, the methane carbon dioxide reforming reaction process was investigated using Ansys Chemkin Pro [39] software. This software is a numerical simulation program specially developed by Kee R.J. et al. of Sandia National Laboratory in 1980 for the design and study of the flow field of chemical reactions, as well as the corresponding gas phase and surface dynamics, and is characterized by its reasonable structure, good reliability, and portability. It has also been validated by many researchers for chemical reaction analysis; therefore, we used Ansys Chemkin Pro in this study to model the methane carbon dioxide reforming thermochemical process.

2.1. Physical Model

Expressions such as the continuity equation, the momentum conservation equation and the energy conservation equation are used as reported in [40].

Continuity equation:

$$\rho u \frac{dA}{dx} + \rho A \frac{d\rho}{dx} + uA \frac{d\rho}{dx} = a_i \sum_{gas}^{k_g} \dot{g}_k W_k \tag{1}$$

Momentum conservation equation:

$$A \frac{dP}{dx} + \rho uA \frac{du}{dx} + \frac{dF}{dx} = ua_i \sum_{gas}^{K_g} \dot{g}_k W_k = 0 \tag{2}$$

Equation of conservation of energy:

$$uA \left(\sum_{gas}^{K_g} h_k \frac{dY_k}{dx} + \overline{C}_P \frac{dT}{dx} + u \frac{du}{dx} \right) + \left(\sum_{gas}^{K_g} h_k Y_k + \frac{1}{2} u^2 \right) a_i \sum_{gas}^{k_g} \dot{g}_k W_k = a_e Q_e - a_i \sum_{bulk}^{K_b} \dot{b}_k W_k h_k \tag{3}$$

Methane conversion rate calculation equation:

$$X_{CH_4} = \frac{CH_{4in} - CH_{4out}}{CH_{4in}} \times 100 \tag{4}$$

2.2. Conditions and Numerical Solution Methods

The boundary conditions of the methane carbon dioxide reforming process include the inlet velocity, the ideal and homogeneously mixed reaction gas, constant the reactor temperature, and the reactor being a tubular reactor. In this paper, the reaction was simulated using Ansys Chemkin Pro. Ansys Chemkin Pro was used to combine the gas phase dynamics data, the thermodynamic database, and to transfer the data to the SPIN module; then, Newton's algorithm was used to solve the coupling problem.

2.3. Model Validation

In order to determine the accuracy of the numerical model of the methane carbon dioxide reforming reaction established in Ansys Chemkin Pro software in this study, we first compared the model results with the results of the methane carbon dioxide reforming surface reaction mechanism reported by Delgado et al. [41] in 2015 using a nickel-based catalyst. The conversion rates of methane and carbon dioxide were calculated at different temperatures, and the error was compared. Comparisons were performed under the same reaction conditions, including using the same size of the reactor model. In Figure 1, the simulation results of this paper are compared with the simulation results found in the literature. Figure 1a presents a comparison of the simulation results reported in this paper with the methane conversion rate described in Ref. [41], while Figure 1b presents a comparison of the simulation results reported in this paper with the carbon dioxide conversion rate described in Ref. [41].

The calculation parameters were as follows: reactor temperature 800–1200 K, inlet gas velocity 4 slpm, and reactor pressure 0.1 MPa. The methane conversion rate in this paper is consistent with the methane conversion trend in the literature, with a maximum error of 7%; therefore, the model described in this paper can be used in future studies.
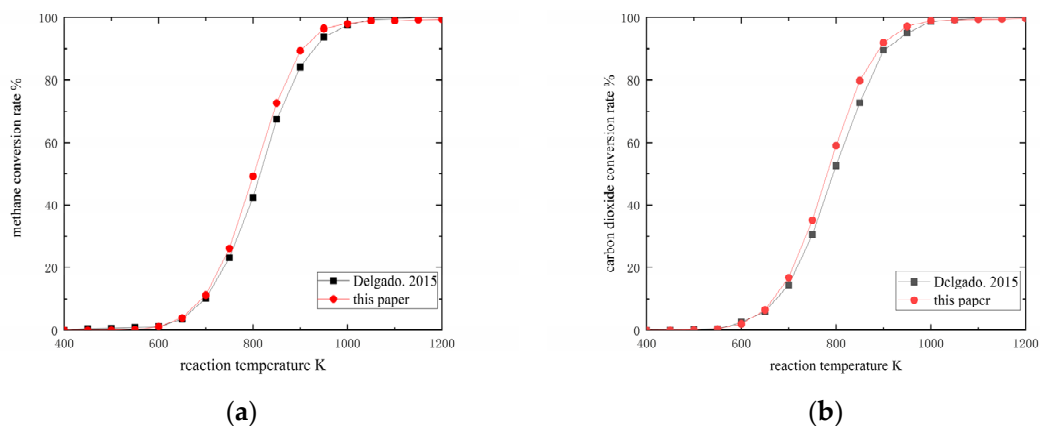
(**a**)   (**b**)

Figure 1. Model validation: (**a**) comparison of the simulation results in this paper with the methane conversion rate reported in Ref. [41]; (**b**) comparison of the simulation results in this paper with the carbon dioxide conversion rate reported in Ref. [41].

3. Results and Discussion

3.1. Single-Factor Simulation Results and Discussion

3.1.1. Influence of Reactor Temperature

Temperature is the most important factor affecting the reaction process in methane carbon dioxide reforming reactions. The methane carbon dioxide reforming reaction equation is shown below, and it can be seen that the reaction is a strong endothermic reaction, and the increase in temperature is conducive to the positive progress of the reaction.

$$CH_4 + CO_2 \rightarrow 2CO + 2H_2 \qquad \Delta H_{298K} = 247.3 \text{ kJ/mol} \qquad (5)$$

Therefore, the conversion rate of methane increases with increasing temperature. The specific change trend is shown in Figure 2, in which the simulated parameters are as follows: reactor temperature, 400–1200 K; CH_4/CO_2, 1; gas flow rate in the reactor, 4 slpm; and reactor pressure, 0.1 MPa. As shown in Figure 2, the methane conversion rate increases with increasing temperature, and the increase in conversion rate in the range 800–1000 K is very significant, but tends to be flat in the range 1000–1200 K. The methane conversion rate of the methane carbon dioxide reforming reaction below 800 K is low, and when the temperature reaches 1200 K, the conversion rate reaches close to 100%, at which point increasing the temperature has little effect on the conversion rate [42]; therefore, the temperature range used in the subsequent response surface method analysis was 800–1200 K.
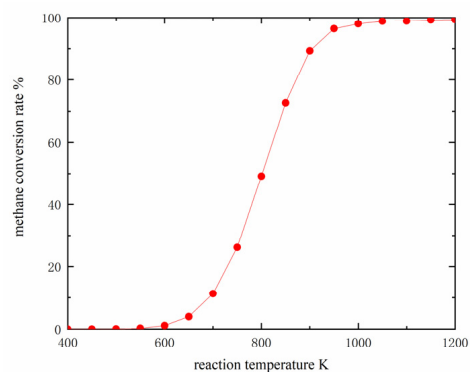

Figure 2. Effect of reactor temperature on methane conversion.

3.1.2. The Effect of Reaction Pressure

Reaction pressure is also one of the important parameters affecting the methane carbon dioxide reforming reaction. On the basis of Le Chatel's principle [43], it can be seen that

when the pressure in the reactor gradually increases, the methane conversion rate of the methane carbon dioxide reforming reaction will decrease, as shown in Figure 3, where the simulation parameters are as follows: reactor temperature, 800–1200 K; CH_4/CO_2, 1; gas flow rate in the reactor, 4 slpm; and reactor pressure, 0.1–3 MPa. The data in Figure 3 show that when the pressure is in the range 0.1–0.5 Mpa, the methane conversion rate of the methane carbon dioxide reforming reaction decreases with increasing pressure, and the reduction rate is at its highest. In the range 0.5–3 Mpa, the rate of reduction of methane conversion gradually decreases and finally flattens. This is because with the progression of the methane carbon dioxide reforming reaction, the amount of gas substances in the reactor continues to increase. The higher the pressure, the higher the methane content in the outlet gas, which reduces methane conversion and hydrogen yield, so the pressure parameters range from 0.1 to 3 MPa.
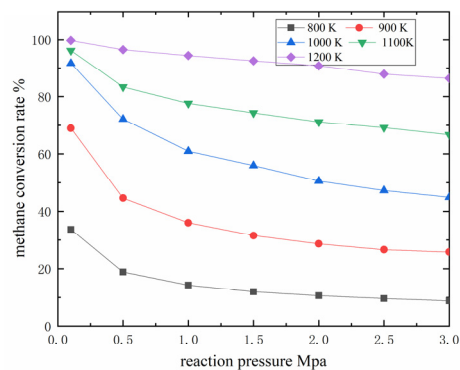

Figure 3. Effect of stress on methane conversion.

3.1.3. Effect of Gas Velocity

Gas velocity is also an important parameter affecting the methane carbon dioxide reforming reaction. The specific effects are shown in Figure 4, where the simulation parameters are as follows: reactor temperature, 800–1200 K; CH_4/CO_2, 1; gas flow rate in the reactor, 1–10 slpm; and reactor pressure, 0.1 MPa. As can be seen from Figure 4, when the temperature is 800–1000 K, the speed has a significant effect on methane conversion. When the temperature is in the range 1100–1200 K, the effect of speed is small. The methane conversion rate decreases with increasing speed, and when the speed is low, the gas flow velocity has a greater effect on the methane conversion rate, but when the speed is high, its influence on methane conversion gradually decreases. This is due to the fact that the greater the gas flow speed, the shorter the stagnant time of the gas in the reactor and the less adequate the reaction. The rate at which methane conversion decreases gradually decreases and eventually flattens out.
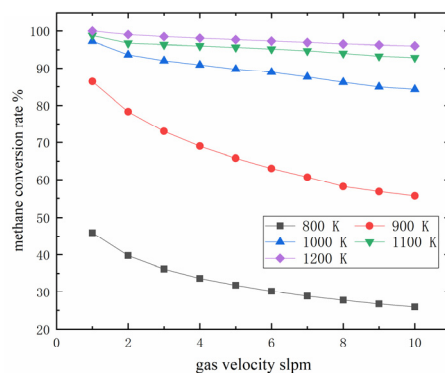

Figure 4. Effect of velocity on methane conversion.

3.2. Response Surface Simulation and Optimization Results

3.2.1. Response Surface Design and Results

Although most scholars start their research on methane carbon dioxide reforming with a single-factor analysis, single-factor analysis alone cannot solve problems in actual production or real-world scenarios. Because various factors often interact, playing their roles at the same time during the experimental stage, simple research on univariate analysis is far from being sufficient. To better be able to achieve the purpose of reducing production costs and improving production efficiency, the response surface method was used to couple the three most important and most influential factors (reaction temperature, reaction pressure, gas velocity) in methane carbon dioxide reforming in order to determine the optimal working conditions of methane carbon dioxide reforming.

The response surface method is a method for performing optimization while reducing the number of experiments required. In this method, the experimental matrix is designed based on criteria for the number of variables and the maximum and minimum limits set for each variable. This allows the number of experiments to be determined, as well as the levels set for each variable in each experiment. This approach facilitates the research process while reducing the time and cost required [44]. In this paper, the BBD model is employed using the response surface methodology to optimize the simulation design of the methane carbon dioxide reforming reaction; the influence of different parameters on the methane conversion rate is studied, and the optimal working condition parameters are selected by the model in order to reach the maximum conversion rate under a comprehensive consideration of the conditions [45]. The effects of temperature (A), pressure (B) and velocity (C) on methane conversion were studied by means of 17 simulations, as shown in Table 1, while Table 2 shows the results obtained for the various parameters, and their changes, in the 17 simulations.

Table 1. Simulation design and response surface results.

Analog Serial Number	Temperature/K	Pressure	Analog Serial Number	Methane Conversion Rate/%
1	800	0.1	5.5	30.9112
2	1000	1.55	5.5	49.9
3	1200	0.1	5.5	99.1042
4	800	3	5.5	8.04932
5	1200	3	5.5	80.911
6	1000	1.55	5.5	49.126
7	1000	0.1	10	83.3062
8	1000	3	10	34.5338
9	1000	1.55	5.5	49.151
10	800	1.55	1	16.6561
11	1200	1.55	1	98.8737
12	800	1.55	10	9.0105
13	1200	1.55	10	81.888
14	1000	1.55	5.5	49
15	1000	0.1	1	99.2649
16	1000	3	1	59.0741
17	1000	1.55	5.5	49.961

Table 2. Variance analysis table of the regression equation.

Source	Sum of Squares	Degrees of Freedom	Mean Squared	F-Value	*p*-Value
Mode	80.72	9	8.97	97.22	<0.0001
A	46.54	1	46.54	504.56	<0.0001
B	17.05	1	17.05	184.42	<0.0001
C	7.95	1	7.95	86.14	<0.0001
AB	0.6647	1	0.6647	7.21	0.0313
AC	1.28	1	1.28	13.89	0.0074
BC	1.31	1	1.31	14.23	0.0070
A^2	0.0704	1	0.0704	0.7631	0.4133
B^2	3.53	1	3.53	38.26	0.0005
C^2	2.08	1	2.08	22.57	0.0021
Residuals	0.6457	7	0.0922		
Misfit	0.5315	3	0.1772	6.20	0.0551
R^2	0.9921				
R^2_{pre}	0.9133				
R^2_{adj}	0.9819				

By fitting the simulation results in the above table using the response surface method, the regression equation between methane conversion (Y_{CH_4}) and pressure (A), temperature (B) and velocity (C) can be obtained (1):

$$Y_{CH_4} = \frac{100}{1 + \alpha} \alpha \tag{6}$$

where α is

$$\alpha = -0.0568 + 2.41 \times A - 1.46 \times B - 0.9966 \times C$$
$$-0.4076 \times AB - 0.5660 \times AC + 0.5729 \times BC - 0.1293 \times A^2 + 0.9155 \times B^2 + 0.7032 \times C^2$$

Typically, ANOVA [46] is used to verify whether the resulting regression equation is feasible, and to verify the significance of the model. The ANOVA results for the regression equations are presented in the table below. In statistical analysis, *p* denotes significance. When the value range of *p* is ≤0.0001, the result is very significant; when the value range of *p* is $0.0001 < p \leq 0.05$, the result is significant; when the value range of *p* is >0.05, the result is insignificant [45,47–49]. It can be seen from the following table that the *p* value of the model is 0.0001, indicating that it is very significant, and the correlation coefficient R^2 between the predicted value and the measured value is 0.9921, indicating that the model is able to explain 99.21% of the variation in response, with a low degree of error. At the same time, the correction coefficient R^2_{adj} and the predicted coefficient R^2_{pre} were both greater than 0.9 and the difference between the two was lower than 0.2, indicating that the selected parameters demonstrate a strong correlation with the response value [50].

In order to more intuitively reflect the influence of multiple factors on methane conversion, the changes in methane conversion under the interaction of three parameters (temperature, pressure, and speed) are depicted in Figure 5. The overall curved surface has a shape with the highest corner (the largest methane conversion ratio) and the lowest corner (the lowest methane conversion ratio). Figure 5a–c show the effect of temperature and pressure, temperature and velocity, and the interaction between pressure and velocity on methane conversion, respectively. It can be seen from Figure 5a that with gradually increasing temperature, the methane conversion rate also increases, and the growth rate goes from high to low. With increasing pressure, the methane conversion rate decreases, and the rate of decline changes from high to low. The change in methane conversion with temperature is more obvious than with pressure, which also indicates that temperature has a stronger effect on methane conversion than pressure. It can be seen from Figure 5b that the methane conversion rate decreases with increasing speed, but this is weaker than the trend

with temperature, indicating that the influence of temperature on methane conversion is still stronger than the influence of speed. It can be seen from Figure 5c that the methane conversion rate decreases with increasing pressure and decreases with increasing speed, but the methane conversion rate decreases more with pressure, so the effect of pressure on methane conversion rate is significantly higher than the effect of speed on hydrogen yield. The degree of influence of the three on the methane conversion rate is in the following order: temperature > pressure > speed. This is also consistent with the results predicted by the regression equation.
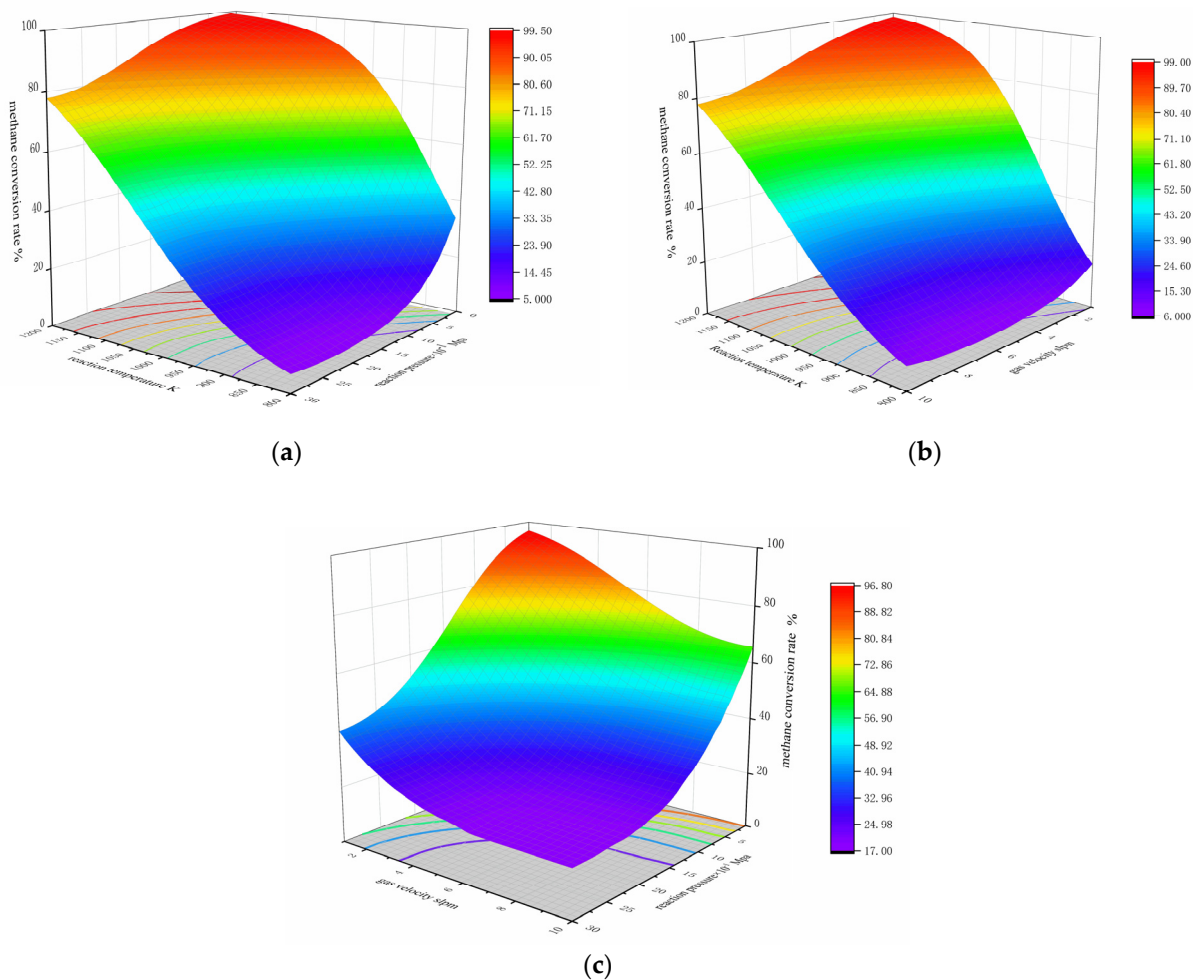

(**a**)

(**b**)

(**c**)

Figure 5. The influence of the interaction of reactor temperature, pressure, and speed on methane conversion: (**a**) effect of reaction temperature and reaction pressure on methane conversion; (**b**) effect of reaction temperature and gas velocity on methane conversion rate; (**c**) effect of reaction pressure and gas velocity on methane conversion.

3.2.2. Analysis of the Response Surface Results

On the basis of the results in the previous section, it is not difficult to conclude that temperature, pressure and speed all have a significant effect on the methane carbon dioxide reforming reaction. When the temperature is lower than 800 K, the methane conversion rate is low, which is not conducive to the occurrence of methane carbon dioxide reforming reaction. When the temperature is higher than 1150 K, the high temperature not only increases the energy consumption of the reaction system, thus increasing the reaction cost, it also shortens the service life of the catalyst. Therefore, an optimized reaction temperature between 800 and 1150 K is selected. It can be seen from Lechatel's principle that the methane carbon dioxide reforming reaction progresses in the direction of increasing the volume of

gas substances, and increasing pressure also increases the requirements in terms of reaction equipment, increased energy consumption and increased costs, so low pressure is more appropriate for the occurrence of the methane carbon dioxide reforming reaction, and the optimal pressure is taken to be about 0.1 Mpa. The increase in gas velocity shortens the time of gas residence in the reactor, and the reaction cannot be fully carried out, which is not conducive to the positive progress of the methane carbon dioxide reforming reaction, but too low a speed will not greatly improve the methane conversion rate, and will also reduce the production efficiency; therefore, an optimal speed value is taken to be 5–15 slpm. In this paper, the Design Expert software package was used to establish a response model with methane conversion as the response value, and a desirability method is used to determine the optimal working conditions [51]. When the working parameters were a temperature of 1135.114 K and a pressure of 0.103 Mpa with a speed of 10 slpm, the desirability of methane conversion was 1, and the predicted maximum value was 94.61%. Combined with the optimized working conditions and simulation parameters, the average value of the results of the three simulations was 93.7018%, and the error was less than 5%, thus proving that the model accuracy is very high, and the optimized parameters are very feasible [52].

4. Conclusions

Based on the simulation of the methane carbon dioxide reforming reaction in Ansys Chemkin Pro tubular reactor, in this paper, different parameters (temperature, pressure and speed) were studied, and the influence of single factors on methane conversion was analyzed. Then, based on a Box–Behnken surface analysis, a quadratic regression equation model between univariate analysis and methane conversion was established, and the working conditions of the methane carbon dioxide reforming reaction were optimized. After the significance of the model had been ascertained on the basis of an analysis of variance, the accuracy of the model was found to be high, and the fit was good.

From the one-way analysis of variance and the interaction response surface analysis, it can be seen that the effects of reaction temperature, reaction pressure and gas flow velocity on the methane conversion rate of the methane carbon dioxide reforming reaction are very significant, with their influence in the following order from high to low: temperature > pressure > velocity. Among them, temperature has a positive effect on methane conversion, while pressure and speed have a negative impact on methane conversion. It can be seen from the univariate analysis results in the previous section that when the reaction temperature is low, the reaction pressure has a greater influence on the methane conversion rate, but with an increase in the reaction temperature, the influence of the reaction pressure on the methane conversion rate is gradually weakened. At the same time, with increasing reaction temperature, the effect of gas velocity on methane conversion demonstrates a similar performance, but it is clear that the influence of gas velocity is more considerably weakened.

It can be found from the response surface analysis that when the desirability is 1, the best working conditions of the methane carbon dioxide reforming reaction are a reaction temperature of 1073.731 K, a reactor pressure of 0.139 Mpa, and a gas flow speed of 6.862 slpm, where the actual value of the methane conversion rate of the reaction of 95.201% and the predicted value of 94.146% basically coincide, indicating that the prediction of the model is highly accurate and can be used for actual prediction.

Author Contributions: Methodology, X.Y.; Formal analysis, Y.W. and S.Z.; Writing—original draft, X.H. and Z.L.; Writing—review & editing, X.Y. and Y.L. All authors have read and agreed to the published version of the manuscript.

Data Availability Statement: No new data were created or analyzed in this study. Data sharing is not applicable to this article.

Conflicts of Interest: The authors declare no conflict of interest.

References

1. IEA. Iron and Steel Technology Roadmap. Available online: https://www.iea.org/reports/iron-and-steel-technology-roadmap (accessed on 2 August 2022).
2. An, R.Y.; Yu, B.Y.; Li, R.; Wei, Y.M. Potential of energy savings and CO_2 emission reduction in China's iron and steel industry. *Appl. Energy* **2018**, *226*, 862–880. [CrossRef]
3. Vogl, V.; Ahman, M.; Nilsson, L.J. Assessment of hydrogen direct reduction for fossil-free steelmaking. *J. Clean. Prod.* **2018**, *203*, 736–745. [CrossRef]
4. Zhang, S.R. Development of Cchinese ironmaking industry after entering the 21* century and the existing problems. In Proceedings of the 6th ECIC, Dusseldorf, Germany, 27 June–1 July 2011; p. 1.
5. Zhang, S.R.; Yin, H. Current Situation and Existing Problems of Blast Furnace Ironmaking in China. *Iron Steel* **2007**, *42*, 1–8.
6. Cavaliere, P. *Spark Plasma Sintering of Materials: Advances in Processing and Applications*; Springer Nature: Basel, Switzerland, 2019; Volume 183, p. 478.
7. Longbottom, R.J.; Kolbeinsen, L. Iron ore reduction with CO and H_2 gas mixtures–Thermodynamic and kinetic modelling. *Fac. Eng. Pap.* **2008**, *4*, 1260.
8. Fan, Z.; Friedmann, S.J. Low-carbon production of iron and steel: Technology options, economic assessment, and policy. *Joule* **2021**, *5*, 829–862. [CrossRef]
9. IEA. The Future of Hydrogen. 2019. Available online: https://www.iea.org/reports/the-future-of-hydrogen (accessed on 2 August 2022).
10. Yuan, Z.; Eden, M.R.; Gani, R. Toward the development and deployment of large-scale carbon dioxide capture and conversion processes. *Ind. Eng. Chem. Res.* **2016**, *55*, 3383–3419.
11. Lu, P.; Xing, C.; Li, H.J.; Gai, X.K.; Wei, Q.H.; Tan, L.; Lu, C.X.; Shen, W.Z.; Yang, R.Q.; Tsubaki, N. An in-situ synthesis of low-cost mesostructured nickel nanoparticles embedded carbon/silica composite via a solid-liquid grinding route and its application for the carbon dioxide reforming of methane. *Int. J. Hydrogen Energy* **2016**, *41*, 10680–10687. [CrossRef]
12. Eliasson, B.; Liu, C.J.; Kogelschatz, U. Direct conversion of methane and carbon dioxide to higher hydrocarbons using catalytic dielectric-barrier discharges with zeolites. *Ind. Eng. Chem. Res.* **2000**, *39*, 1221–1227. [CrossRef]
13. Oberreuther, T.; Wolff, C.; Behr, A. Volumetric plasma chemistry with carbon dioxide in an atmospheric pressure plasma using a technical scale reactor. *IEEE Trans. Plasma Sci.* **2003**, *31*, 74–78. [CrossRef]
14. Moradi, K.; Depecker, C.; Barbillat, J.; Corset, J. Diffuse reflectance infrared spectroscopy: An experimental measure and interpretation of the sample volume size involved in the light scattering process. *Spectrochim. Acta Part A* **1999**, *55*, 43–64. [CrossRef]
15. Song, Y.; Ozdemir, E.; Ramesh, S.; Adishev, A.; Subramanian, S.; Harale, A.; Albuali, M.; Fadhel, B.A.; Jamal, A.; Moon, D.; et al. Dry reforming of methane by stable Ni-Mo nanocatalysts on single-crystalline MgO. *Science* **2020**, *367*, 777–781. [CrossRef] [PubMed]
16. Yentekakis, I.V.; Goula, G.; Hatzisymeon, M.; Betsi-Argyropoulou, I.; Botzolaki, G.; Kousi, K.; Kondarides, D.I.; Taylor, M.J.; Parlett, C.M.A.; Osatiashtiani, A.; et al. Effect of support oxygen storage capacity on the catalytic performance of Rh nanoparticles for CO_2 reforming of methane. *Appl. Catal. B Environ.* **2019**, *243*, 490–501. [CrossRef]
17. Pakhare, D.; Spivey, J. A review of dry (CO_2) reforming of methane over noble metal catalysts. *Chem. Soc. Rev.* **2014**, *43*, 7813–7837. [CrossRef] [PubMed]
18. Zhang, G.; Liu, J.; Xu, Y.; Sun, Y. A review of CH_4 CO_2 reforming to synthesis gas over Ni-based catalysts in recent years (2010–2017). *Int. J. Hydrogen Energy* **2018**, *43*, 15030–15054. [CrossRef]
19. Aramouni, N.A.K.; Touma, J.G.; Tarboush, B.A.; Zeaiter, J.; Ahmad, M.N. Catalyst design for dry reforming of methane: Analysis review. *Renew. Sustain. Energy Rev.* **2018**, *82*, 2570–2585. [CrossRef]
20. Abdulrasheed, A.; Jalil, A.A.; Gambo, Y.; Ibrahim, M.; Hambali, H.U.; Hamid, M.Y.S. A review on catalyst development for dry reforming of methane to syngas: Recent advances. *Renew. Sustain. Energy Rev.* **2019**, *108*, 175–193. [CrossRef]
21. Akri, M.; Zhao, S.; Li, X.; Zang, K.; Lee, A.F.; Isaacs, M.A.; Xi, W.; Gangarajula, Y.; Luo, J.; Ren, Y.; et al. Atomically dispersednickel as coke resistant active sites for methane dry reforming. *Nat. Commun.* **2019**, *10*, 5181. [CrossRef]
22. Charisiou, N.D.; Siakavelas, G.; Tzounis, L.; Sebastian, V.; Monzon, A.; Baker, M.A.; Hinder, S.J.; Polychronopoulou, K.; Yentekakis, I.Y.; Goula, M.A. An in depth investigation of deactivation through carbon formation during the biogas dry reforming reaction for Ni supported on modified with CeO_2 and La_2O_3 zirconia catalysts. *Int. J. Hydrogen Energy* **2018**, *43*, 18955–18976. [CrossRef]
23. Cui, Y.; Liu, Q.; Yao, Z.; Dou, B.; Shi, Y.; Sun, Y. A comparative study of molybdenum phosphide catalyst for partial oxidation and dry reforming of methane. *Int. J. Hydrogen Energy* **2019**, *44*, 11441–11447. [CrossRef]

24. Ma, H.; Yang, J.Y.; Zhang, F.; Li, H.; Li, H.; Yang, Z.Q. Analysis on deactivation of hydrocracking catalyst for industrial Fischer-Tropsch synthetic oil. *Low-Carbon Chem. Chem. Eng.* **2022**, *47*, 1–7.

25. Gao, Y.J. Study on the Performance of Composite Oxide Catalysts in Fischer-Tropsch Synthesis of Light Olefins. Master's Thesis, Zhengzhou University of Light Industry, Zhengzhou, China, 2022.

26. Kumari, R.; Sengupta, S. Catalytic CO_2 reforming of CH_4 over $MgAl_2O_4$ supported Ni-Co catalysts for the syngas production. *Int. J. Hydrogen Energy* **2020**, *45*, 22775–22787. [CrossRef]

27. Li, X.Y.; Li, D.; Tian, H.; Zeng, L.; Zhao, Z.J.; Gong, J.L. Dry reforming of methane over Ni/La_2O_3 nanorod catalysts with stabilized Ni nanoparticles. *Appl. Catal. B* **2017**, *202*, 683–694. [CrossRef]

28. Chen, L.; Qi, Z.; Zhang, S.; Su, J.; Somorjai, G.A. Catalytic Hydrogen Production from Methane: A Review on Recent Progress and Proszect. *Catalysts* **2022**, *10*, 858. [CrossRef]

29. Shamsuddin, M.R.; Asikin-mijan, N.; Saiman, M.I.; Tengku, S.M.; Yarmo, M.A.; Taufiq-Yap, Y.H. Evaluation of NiO/TALC catalytic performance in carbon dioxide reforming of methane. *J. Taiwan Inst. Chem. Eng.* **2021**, *122*, 106–117. [CrossRef]

30. Lin, L.I.; Zhang, L.M.; Zhang, Y.H.; Li, J.L. Effect of Ni loadings on the catalytic properties of Ni/MgO(111) catalyst for the reforming of methane with carbon dioxide. *J. Fuel Chem. Technol.* **2015**, *43*, 315–322.

31. Jing, J.Y.; Wei, Z.H.; Zhang, Y.B.; Bai, H.C.; Li, W.Y. Carbon dioxide reforming of methane over MgO-promoted Ni/SiO_2 catalysts with tunable Ni particle size. *Catal. Today* **2020**, *356*, 589–596. [CrossRef]

32. Jeong, H.; Kim, K.I.; Kim, D.; Song, I.K. Effect of promoters in the methane reforming with carbon dioxide to synthesis gas over Ni/HY catalysts. *J. Mol. Catal. A Chem.* **2006**, *246*, 43–48. [CrossRef]

33. Nikoo, M.K.; Amin, N.A.S. Thermodynamic analysis of carbon dioxide reforming of methane in view of solid carbon formation. *Fuel Process. Technol.* **2011**, *92*, 678–691. [CrossRef]

34. Janardhanan, V.M.; Deutschmann, O. CFD analysis of a solid oxide fuel cell with internal reforming: Coupled interactions of transport, heterogeneous catalysis and electrochemical processes. *J. Power Sources* **2006**, *162*, 1192–1202. [CrossRef]

35. Özkara-Aydınoğlu, Ş. Thermodynamic equilibrium analysis of combined carbon dioxide reforming with steam reforming of methane to synthesis gas. *Int. J. Hydrogen Energy* **2010**, *35*, 12821–12828. [CrossRef]

36. Hettel, M.; Diehm, C.; Bonart, H.; Deutschmann, O. Numerical simulation of a structured catalytic methane reformer by DUO: The new computational interface for OpenFOAM® and DETCHEM™. *Catal. Today* **2015**, *258*, 230–240. [CrossRef]

37. Fuqiang, W.; Lin, J.; Ziming, C.; Huaxu, L.; Jianyu, T. Combination of thermodynamic analysis and regression analysis for steam and dry methane reforming. *Int. J. Hydrogen Energy* **2019**, *44*, 15795–15810. [CrossRef]

38. Lanhua, Z.; Fuhong, Z.; Yongmin, G. Optimization of Separating Iron and Zinc from BF Gas Sludge by BBD Method. Multipurp. *Util. Miner. Resour.* **2022**, *43*, 31–36.

39. Ansys Chemkin-Pro Overview, Retrieved. Available online: https://www.ansys.com/training-center/course-catalog/fluids/introduction-to-ansys-chemkin-pro. (accessed on 25 July 2022).

40. Larson, R.S. *PLUG: A Fortran Program for the Analysis of PLUG Flow Reactors with Gas-Phase and Surface Chemistry*; Sandia Labs: Livermore, CA, USA, 1996. [CrossRef]

41. Delgado, K.H.; Maier, L.; Tischer, S.; Zellner, A.; Stotz, H.; Deutschmann, O. Surface reaction kinetics of steam-and CO_2-reforming as well as oxidation of methane over nickel-based catalysts. *Catalysts* **2015**, *5*, 871–904. [CrossRef]

42. Dalin, L.; Nakagawa, Y.; Tomishige, K. Methane reforming to synthesis gas over Ni catalysts modified with noble metals. *Appl. Catal. A* **2011**, *408*, 1–24.

43. Zhu, Y.H.; Mao, G.L.; Fan, S. The thermodynamic basis of Lechatel's principle and its related controversial issues. *Educ. Chem.* **2020**, *12*, 88–91.

44. Jensen, W.A. Response Surface Methodology: Process and product optimization using designed experiments. *J. Qual. Technol.* **2017**, *42*, 186. [CrossRef]

45. Rahimi, M.; Aghel, B.; Alitabar, M.; Sepahvand, A.; Ghasempour, H.R. Optimization of biodiesel production from soybean oil in a microreactor. *Energy Convers. Manag.* **2014**, *79*, 599–605. [CrossRef]

46. Ayodele, B.V.; Ghazali, A.A.; Yassin, M.Y.M.; Abdullah, S. Optimization of hydrogen production by photocatalytic steam methane reforming over lanthanum modified Titanium (IV) oxide using response surface methodology. *Int. J. Hydrogen Energy* **2019**, *44*, 20700–20710. [CrossRef]

47. Yang, Z.H.; Huang, J.; Zeng, G.M.; Ruan, M.; Zhou, C.S.; Li, L.; Rong, Z.G. Optimization of flocculation conditions for Kaolin suspension using the composite flocculant of MBFGA1 and PAC by response surface methodology. *Bioresour. Technol.* **2009**, *100*, 4233–4239. [CrossRef]

48. Alenyorege, E.A.; Ma, H.; Aheto, J.H.; Ayim, I.; Chikari, F.; Osae, R.; Zhou, C. Response surface methodology centred optimization of mono-frequency ultrasound reduction of bacteria in fresh-cut Chinese cabbage and its effect on quality. *LWT* **2020**, *122*, 108991. [CrossRef]

49. Hao, C.L.; Guo, J.Y.; Chu, M.; Yan, Y.B.; Wang, L.S.; Gong, Y.Q.; Zhao, X.P. Analysis of models and factors of long flame coal flotation process by response surface methodology. *J. Min. Sci. Technol.* **2019**, *4*, 547–557.

50. Fan, M.S.; Abdullah, A.Z.; Bhatia, S. Hydrogen production from carbon dioxide reforming of methane over $Ni–Co/MgO–ZrO_2$ catalyst: Process optimization. *Int. J. Hydrogen Energy* **2011**, *36*, 4875–4886. [CrossRef]

51. Ferreira, S.L.C.; Bruns, R.E.; Ferreira, H.S.; Matos, G.D.; David, J.M.; Brandão, G.C.; da Silva, E.G.P.; Portugal, L.A.; dos Reis, P.S.; Souza, A.S.; et al. Box-Behnken design: An alternative for the optimization of analytical methods. *Anal. Chim. Acta* **2007**, *597*, 179–186. [CrossRef]
52. Liu, Y.; Zhou, M.; Zhang, K.; Wu, L.; Peng, L. The optimization of pervious concrete ratios with spontaneous combustion gangue aggregates based on the RSM-BBD method. *J. Min. Sci. Technol.* **2022**, *7*, 565–576.